

DIAGNOSIS METHOD FOR GTO OPEN SWITCH FAULT APPLIED TO RECONFIGURABLE THREE-LEVEL 48-PULSE STATCOM

Omar Fethi BENAOUA^{1,2}, Azzedine BENBIABDELLAH², Bilal Djamal Eddine CHERIF²

¹Research Center in Industrial Technologies CRTI, P.O.Box 64, Cheraga 16014, Algiers, Algeria

²Diagnostic Group, LDEE laboratory, Electrical Engineering Faculty, University of Sciences and Technology of Oran MB, BP 1505 El-Mnaouer, Oran 31000, Algeria

o.benaouda@crti.dz, Benaouda.omar@gmail.com, bendiazz@yahoo.fr, cherif.doc84@gmail.com

DOI: 10.15598/aeec.v17i2.3192

Abstract. *In the recent years, several research works are focusing on the use of STATCOM in electrical networks because it is used to regulate the voltage, to improve the dynamic stability of the power system besides allowing better management of the power flow. All these positive tasks have guaranteed an important position of STATCOM within a family of Flexible Alternating Current Transmission System (FACTS). In this paper study, the control and operation of a three levels 48-pulse GTO based STATCOM is implemented with series connected transformers. The system may, unfortunately, be prone to GTO switch faults and therefore may affect reactive power transiting. In this paper, a new diagnostic approach is proposed based on the Single-Sided Amplitude Spectrum (SSAS) method of the three-leg converter currents for detection and localization of open-circuit faults. The integration of the STATCOM reconfigurable fault tolerant to the system is also considered to ensure service continuity. Several results are presented and discussed in this paper to illustrate the performance of the STATCOM fault-tolerant diagnostic.*

Keywords

Detection, diagnosis, FACTS, GTO, open switch fault, reconfiguration, SSAS, STATCOM.

1. Introduction

The systems of Flexible Alternating Current Transmission (FACTS) have become available worldwide due to the growing demand for energy; these systems gener-

ally use power electronics. There are two main trends in the future outlook on the concept of the development of electrical networks; either to improve the quality of the electrical networks or to strengthen these networks [1]; the latter is not an economical solution, the solution is therefore in improving the networks. The use of Flexible AC Transmission Systems (FACTS) has significantly contributed to enhancing both the voltage control and the network stability and hence allowing better management of the power flow [2]. The basic principle of the STATic COMPensator (STATCOM) is in its ability to generate and absorb reactive power between the AC system and the STATCOM [3] and [4]. This is possible thanks to the topology structure of the power electronics converter which often depends on the high-power compensators due to its operating efficiency [5], [6], [7], [8] and [9]. The three-level power converter is the most popular multi-level topology used in the various industrial applications [10]; these converters are particularly used in the FACTS systems which contain GTO thyristor switches since they enable high power management capability. The use of a large number of the structural semiconductor switches is in fact very important in increasing the converter capability according to the required power levels, but is unfortunately reflected negatively by the increase in the converter structure complexity on the one hand and in increasing the possibility of the exposure to faults in the converter on the other hand [11].

In electrical systems that include power converters, several faults may appear in the converter, on its switch control [12] or in the physical semiconductor component itself [13]. Many research concerns are about the behaviour study of the converter; especially after the occurrence of a fault in the semiconductor components or a driver fault [14] and [15]. In the STATCOM sys-

tem, the converter has two operating modes; either as a rectifier or an inverter; in accordance with the source of the voltage change. These devices are very sensitive to a fault in terms of reliability and therefore the detection and localization of faults become a necessity and are the most profitable. Thus, in order to ensure planned maintenance or improve reliability, diagnostic and fault detection methods must be applied. In general, the faults can be classified as short-circuit faults and open-circuit faults [16] and [17]. Some diagnostic methods have been developed for converters in the last decade by many researchers like Mendes, Abramik, Peugeot and all [18] and [19].

In the case of open-circuit faults, most of these fault diagnostic methods for inverters have been reviewed by Bin Lu [20] and [21], while a few researchers take care to study the diagnosis of the three-phase rectifier [22]. At this stage, it should be noted that it is somehow difficult to apply diagnostic techniques on the STATCOM system because the converter may work either as a rectifier or an inverter and it is possible that the switching from one mode to another may occur at any time.

There is a number of researchers that have gone beyond the diagnosis and detection tasks by introducing the concept of fault tolerance in the design of converter topologies. To maintain the continuity of service of the converter with an acceptable performance after the fault occurrence, either reconfiguration based on redundancy or control techniques are applied to the converter [23]. The three-level converter is considered to be one of the most famous of tolerant topologies described in the literature [24]. There are many techniques to reconfigure the converter; either by adding an extra (or redundant) leg or by changing or readapting the control of the healthy legs. This tolerance is achieved by adding some devices to the fundamental topology.

This paper proposes a diagnostic technique based mainly on the method of calculating Single-Sided Amplitude Spectrum (SSAS) for the GTO open-circuit fault in the three-level converter operating under the two modes; rectifier or inverter.

First, a comparison of the GTO switch opening fault is indicated in the STATCOM. Subsequently, the methods for diagnosing SSAS faults are applied and then proposed to the STATCOM converters. Finally, A multi-level fault tolerant converter is incorporated in the system and discussions about the effects of an open-circuit fault on the entire system ± 100 MVAR 48-pulse GTO STATCOM is presented.

2. System Description

Figure 1 depicts the 48-pulse GTO STATCOM configuration which is composed of four converters (Conv1, Conv2, Conv3 and Conv4) where each one of them has its own switching frequency. These converters are connected in series with four transformers (Trans1, Trans2, Trans3 and Trans4). The phase shifts of the four transformers are -15° , -7.5° , $+7.5^\circ$ and $+15^\circ$, respectively. The voltages obtained on the 500 kV sides of the transformers are connected in phase after the series connection of the primary windings, where the STATCOM has behaviour according to the relation voltage generated by the component of voltage source converter with the system voltage.

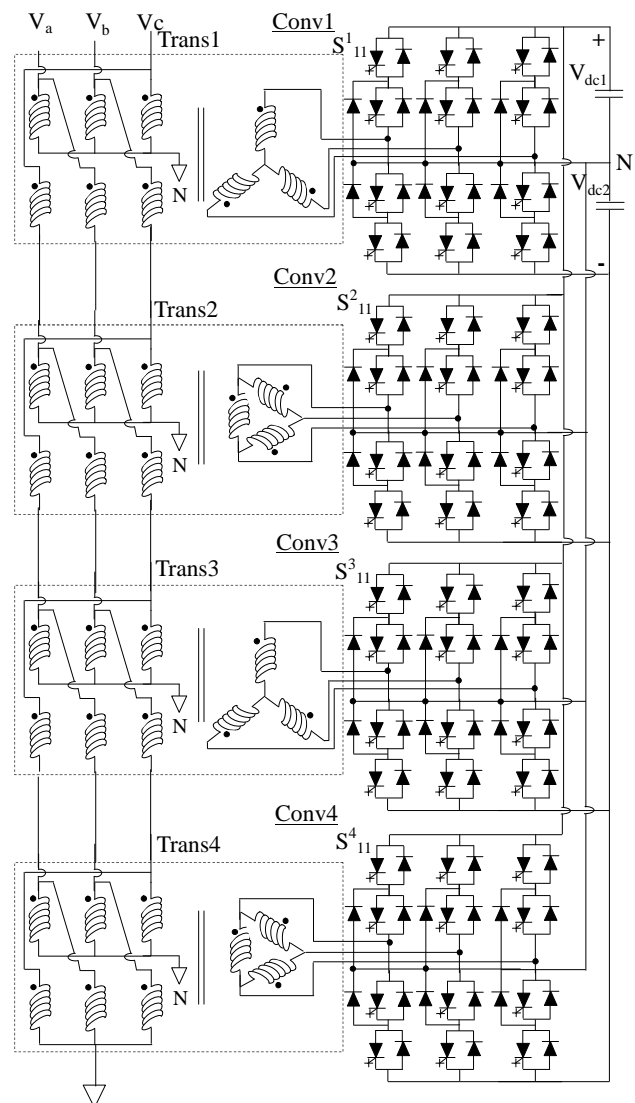


Fig. 1: Three-level 48-Pulse STATCOM system configuration (± 100 MVA).

If the STATCOM is operating in a steady state, this means that there is parity between the Voltage-Sourced Converter (VSC) and the system voltage, but if they are not equal, the STATCOM will intervene either to absorb or generate reactive power.

In order to know the dynamic response of the STATCOM with respect to changes in the system voltage, one of the three voltage sources used can be modified. Figure 1 shows the three-level 48-Pulse STATCOM system configuration.

The phase shift expression of each 12-pulse converter is defined as follows: The 12-pulse compound voltage generated by each of the four converters are given as:

The first 12-Pulse Converter (Conv1):

$$\begin{aligned} V_{ab12}(t)_1 = & \\ & 2[V_{ab1} \sin(\omega t + 30^\circ) + V_{ab11} \sin(11\omega t + 195^\circ) \\ & + V_{ab13} \sin(13\omega t + 255^\circ) + V_{ab23} \sin(23\omega t + 600^\circ) \\ & + V_{ab25} \sin(25\omega t + 120^\circ) + \dots] \end{aligned} \quad (1)$$

The second 12-Pulse Converter (Conv2):

$$\begin{aligned} V_{ab12}(t)_2 = & \\ & 2[V_{ab1} \sin(\omega t + 30^\circ) + V_{ab11} \sin(11\omega t + 15^\circ) \\ & + V_{ab13} \sin(13\omega t + 75^\circ) + V_{ab23} \sin(23\omega t + 60^\circ) \\ & + V_{ab25} \sin(25\omega t + 120^\circ) + \dots] \end{aligned} \quad (2)$$

The third 12-Pulse Converter (Conv3):

$$\begin{aligned} V_{ab12}(t)_3 = & \\ & 2[V_{ab1} \sin(\omega t + 30^\circ) + V_{ab11} \sin(11\omega t + 285^\circ) \\ & + V_{ab13} \sin(13\omega t + 345^\circ) + V_{ab23} \sin(23\omega t + 240^\circ) \\ & + V_{ab25} \sin(25\omega t + 300^\circ) + \dots] \end{aligned} \quad (3)$$

The fourth 12-Pulse Converter (Conv4):

$$\begin{aligned} V_{ab12}(t)_4 = & \\ & 2[V_{ab1} \sin(\omega t + 30^\circ) + V_{ab11} \sin(11\omega t + 105^\circ) \\ & + V_{ab13} \sin(13\omega t + 165^\circ) + V_{ab23} \sin(23\omega t + 240^\circ) \\ & + V_{ab25} \sin(25\omega t + 300^\circ) + \dots] \end{aligned} \quad (4)$$

The output voltage of the 48-pulse neutral line from the STATCOM model is expressed by:

$$\begin{aligned} V_{an48}(t) = & \\ & \sum_{n=1}^{\infty} V_{abn} \sin(n\omega t + 18.75^\circ n + 18.75^\circ i) \quad (5) \\ & \forall n = 48r \pm 1, \quad r = 0, 1, 2, \dots \end{aligned}$$

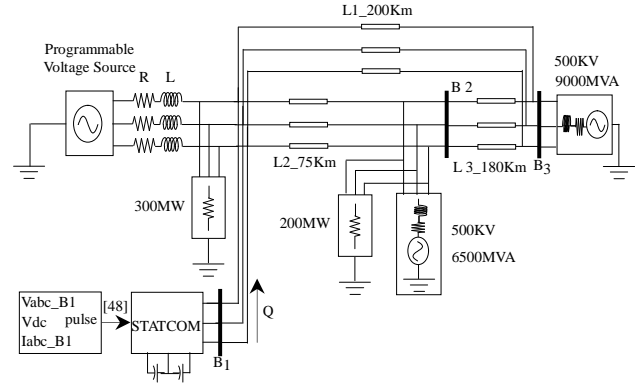


Fig. 2: System simulation with a 48-pulse VSC based ± 100 MVAR STATCOM in a 3-bus power system.

2.1. Simulation Results and Discussions

In the following section, some simulation results of the healthy STATCOM using the MATLAB/ SIMULINK environment are obtained and discussed. The simulation results depicted in Fig. 3 show the dynamic response of a healthy STATCOM for the source voltage change. The programmable voltage source is changed to determine the reaction of the STATCOM. It is important to note that before the instant 0.05 s, the source voltage equals 1 pu, while the secondary voltage V_{sa} of the bus B1 equals 1 pu and the primary current $I_{a\text{ Prim}}$ takes the value 0 pu.

This situation indicates in fact, the non-intervention of the STATCOM; the DC voltage equals 1 pu and the reactive power is stable to its value of zero. After that instant, the source voltage decreases to the value of 0.979 pu hence allowing the intervention of the STATCOM to generate 70 MVAR of the reactive power with a dynamic response time equals to 47 ms. At this point, the DC voltage has increased to 1.07 pu, the primary current $I_{a\text{ Prim}}$ is advanced by supplying the voltage of bus B1. At the instant 0.15 s, the source voltage is increased to 1.025 pu of its nominal value, which makes the STATCOM absorbs 40 MVAR of reactive power and the value of DC voltage decreases to 0.97 pu. At the instant 0.25 s, the source voltage is equal to 1 pu which implies the non-intervention of the STATCOM and therefore proving that the reactive power is equal to 0 MVAR.

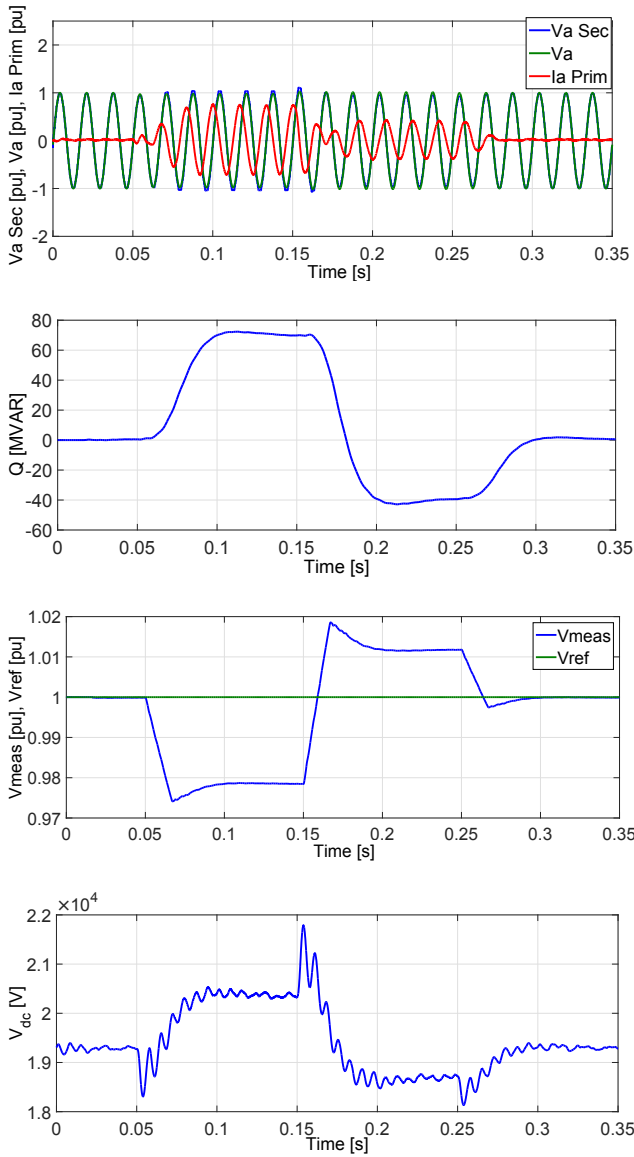


Fig. 3: Healthy STATCOM dynamic response waveforms related to the system voltage change.

3. STATCOM Under Open Switch Fault

3.1. GTO Open-Circuit Fault of the Conv1

In order to study the effect of the fault on the behaviour of the STATCOM, an open-circuit fault at the switch S^{1}_{12} in the conv1 is created at the instant $t = 0.12$ s; see Fig. 4. As for the rest of the converters, they are supposed to remain all healthy.

In reference to Fig. 5, it can be observed that the open-circuit fault does not affect directly the voltage V_a but it affects significantly the current I_a Prim as a result of the distortions (harmonics). It can be noticed

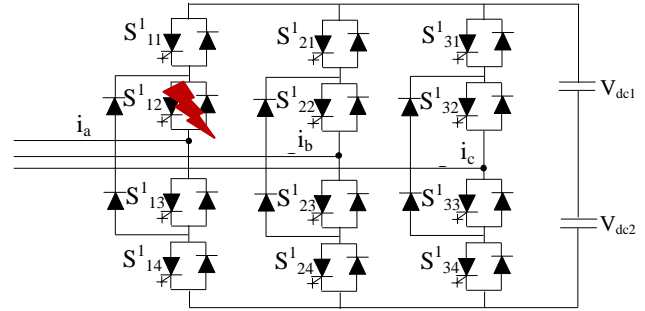


Fig. 4: Conv1 with open switch fault.

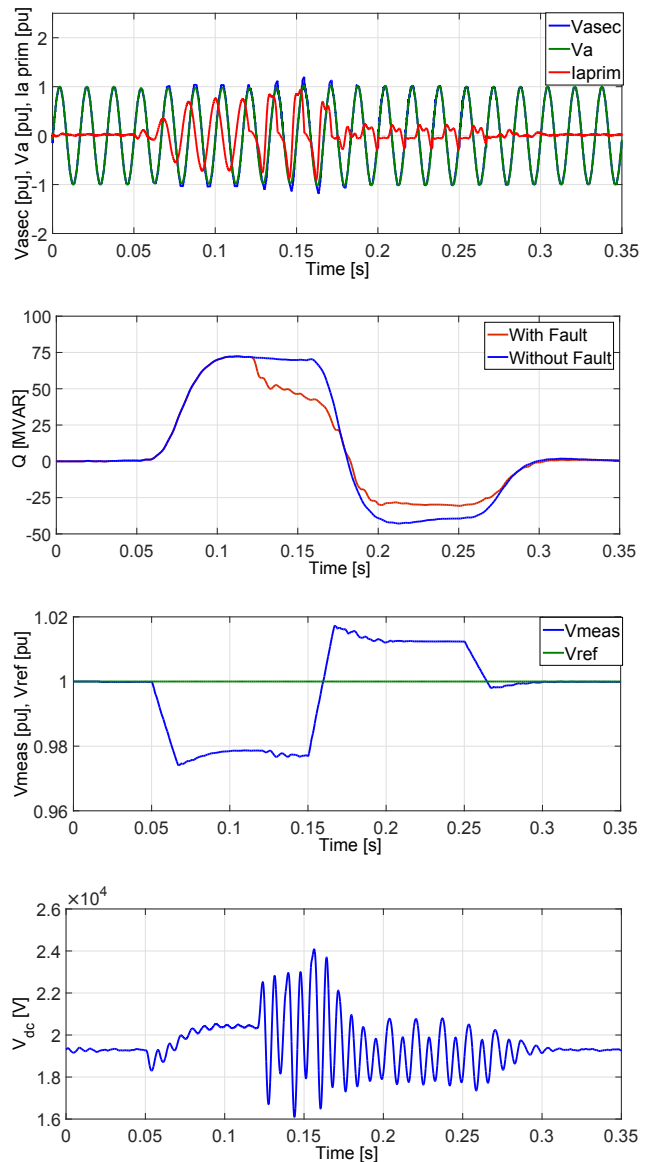


Fig. 5: Faulty STATCOM dynamic response waveforms related to the system voltage change, (Case of a Conv1 GTO open-circuit fault at the instant of 0.12 s).

that after the fault occurrence, the reactive power flow increases in the inductive mode but decreases when the STATCOM is operating in the capacitive mode. It can

also be seen that many perturbations appear on the DC voltage. Before proceeding with the removal of these fault effects, one must rely on the diagnostic method that enables detecting the faults and their localization. The current signals are used in this paper study as they help well in the diagnosis and the detection of the faults.

4. Method of Detection and Localization of Open-Circuit Faults

In this section, the use of an adopted diagnostic method called the Single-Sided Amplitude Spectrum (SSAS) method is proposed to detect and localize open-circuit fault applied to STATCOM converters. The novelty of this work lies in the fact that the proposed SSAS method previously used in signal processing applications is applied for the first time in the field of diagnosis of converters and more particularly in the STATCOM converters diagnosis applications.

The important advantage of the SSAS method compared to Park vectors method, for example, is that it has the ability to diagnose each phase on its own hence facilitating the detection and localization process, especially in the case of faults in the two operations (capacitive or inductive). The results obtained using the SSAS method depict well its merits and effectiveness.

4.1. Fault Detection of the Faulty Leg by the SSAS

Spectral analysis is a technique widely used in signal processing; it consists of transposing the signal from the time-space to the frequency-space [25] and [26]. The spectral representation is obtained by the Fourier transform which was first introduced by Joseph Fourier. The Fourier transform $S(f)$ of a signal $s(t)$ is given by the following equation:

$$I_{a,b,c}(f) = \int_{-\infty}^{\infty} i_{a,b,c}(t)e^{-j2\pi ft} dt. \quad (6)$$

The positive aspect of this technique is that it is based on the study of the harmonic analysis of each phase current and differs from the Park vectors method which depends on the transformation of the three-phase currents to the two d - q currents in the d - q axis frame [27].

4.2. Results Discussion

In this case, the SSAS method is applied to the three-level converter conv1 currents under the healthy condition. This diagnostic method consists of calculating the amplitude spectrum at the fundamental frequency. Figure 6 shows the spectral analysis in the case of a healthy state of the three legs currents (i_{ai} , i_{bi} , i_{ci}) for the inverter and (i_{ar} , i_{br} , i_{cr}) for the rectifier, the amplitude of the fundamental spectrum is equal 106 % in both operating modes. In Fig. 7, it is noticed that during the occurrence of an open-circuit fault introduced in the conv1 S^1_{12} switch when operating in the capacitive mode, the spectral amplitude of the current of the first faulty leg $I_{ai}(f)$ is equal to 16 %. For the remaining healthy legs, the value of $I_{ai}(f)$ is greater than or equal to 120 %. In the inductive operating mode, the value of $I_{ar}(f)$ of the first faulty leg is equal to 50 %. For the other healthy legs, $I_{ar}(f)$ is greater than or equal to 120 %.

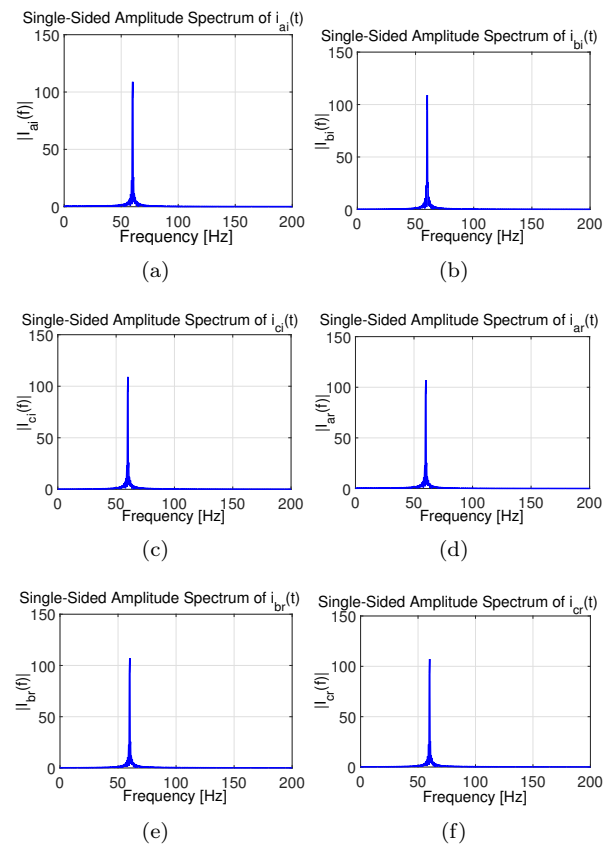


Fig. 6: Simulation results of spectral analysis of three currents of healthy conv1, under two operating modes: ((a), (b), (c)): capacitive and ((d), (e), (f)): inductive.

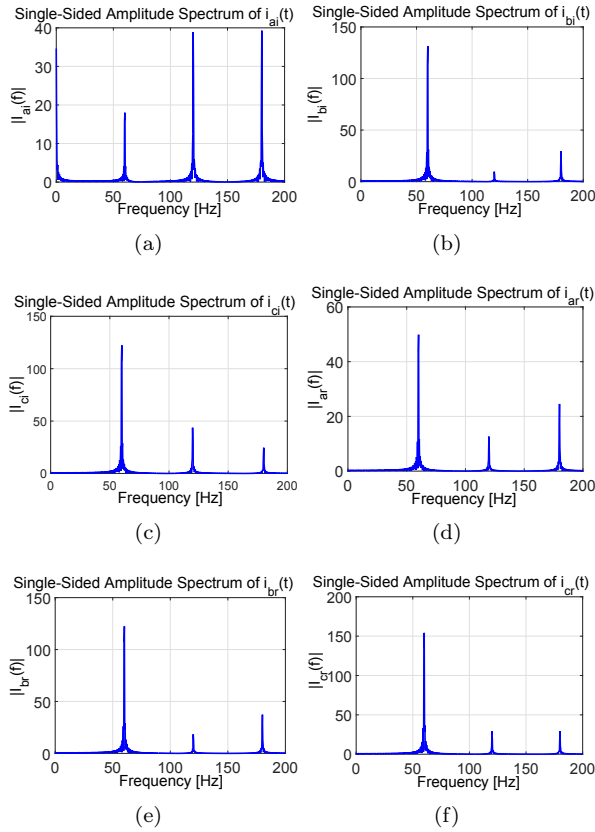


Fig. 7: Simulation results of spectral analysis of three currents with an open-circuit fault introduced in conv1 GTO S^{1}_{12} switch under two operating modes: ((a), (b), (c)): capacitive and ((d), (e), (f)): inductive.

4.3. Fault Localization of the Faulty Open-Circuit Switch

After discovering the faulty leg by applying the SSAS method, in order for the diagnosis to be completed, the faulty switch should be located, for that, this method is deepened in reading the signal of spectral analysis of phase currents.

4.4. Simulation Results

Each time an open-circuit fault is created at one switch in the first leg, then the value of $|I_a S^1_{xy}(f)|$ is calculated in the two operating modes as illustrated in Fig. 8. Through the spectra depicted in Fig. 8, it can be concluded that the fundamental amplitude of the spectrum $|I_a S^1_{xy}(f)|$ of the phase current helps to localize the open-circuit faults in any switch because this value is reduced in the case of a fault occurrence, where each faulty switch has a certain value of $|I_a S^1_{xy}(f)|$. The following table shows the values of $|I_a S^1_{xy}(f)|$ under the two operating modes.

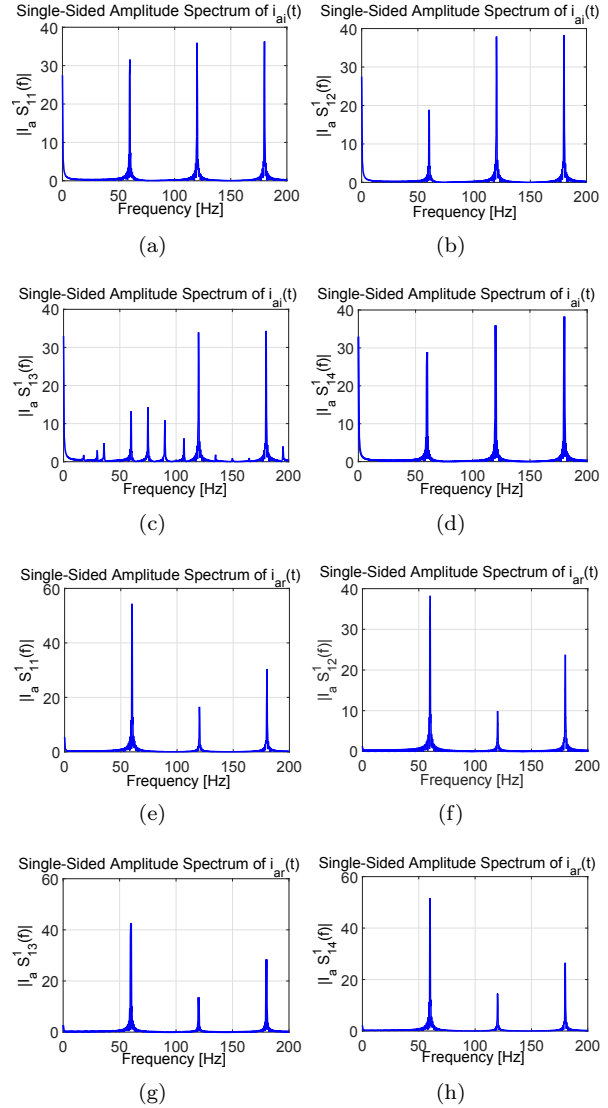


Fig. 8: Simulation results of spectral analysis of phase current i_a with an open-circuit fault introduced in switches (S^{1}_{11} , S^{1}_{12} , S^{1}_{13} , S^{1}_{14}) of conv1 GTO switch, under two operating modes: capacitive ((a), (b), (c), (d)) and inductive ((e), (f), (g), (h)).

Tab. 1: Amplitude of the fundamental spectrum.

Operation	$ I_a S^1_{xy}(f) $			
	S^{1}_{11}	S^{1}_{12}	S^{1}_{13}	S^{1}_{14}
Capacitive	30 %	16 %	13 %	27 %
Inductive	55 %	38 %	43 %	50 %

Table 1 summarizes the characteristics of the various faults of the GTO switch in the conv1. Since Tab. 2 below is large, the values of $|I_a S^1_{xy}(f)|$ are replaced by the value of A_{Fa} . It is important to note that the lower the value of $|I_a S^1_{xy}(f)|$, the fault effect is increased and is more sensitive when the faulty STATCOM is under the capacitive operating mode compared to the inductive operating mode.

Tab. 2: Characteristics of the different open-circuit GTO switch faults in conv1.

States	Leg1	Leg2	Leg3
Capacitive Operation			
No fault	$A_{Fa} = I_{ai} $	$A_{Fb} = I_{bi} $	$A_{Fc} = I_{ci} $
S^1_{11} open	$ I_{ai} _{in} < A_{Fa} < I_{ai} $	$A_{Fb} > I_{bi} $	$A_{Fc} > I_{ci} $
S^1_{12} open	$A_{Fa} < I_{ai} _{ex}$	$A_{Fb} > I_{bi} $	$A_{Fc} > I_{ci} $
S^1_{13} open	$A_{Fa} < I_{ai} _{ex}$	$A_{Fb} > I_{bi} $	$A_{Fc} > I_{ci} $
S^1_{14} open	$ I_{ai} _{in} < A_{Fa} < I_{ai} $	$A_{Fb} > I_{bi} $	$A_{Fc} > I_{ci} $
S^1_{21} open	$A_{Fa} > I_{ai} $	$ I_{bi} _{in} < A_{Fb} < I_{bi} $	$A_{Fc} > I_{ci} $
S^1_{22} open	$A_{Fa} > I_{ai} $	$A_{Fb} < I_{bi} _{ex}$	$A_{Fc} > I_{ci} $
S^1_{23} open	$A_{Fa} > I_{ai} $	$A_{Fb} < I_{bi} _{ex}$	$A_{Fc} > I_{ci} $
S^1_{24} open	$A_{Fa} > I_{ai} $	$ I_{bi} _{in} < A_{Fb} < I_{bi} $	$A_{Fc} > I_{ci} $
S^1_{31} open	$A_{Fa} > I_{ai} $	$A_{Fb} > I_{bi} $	$ I_{ci} _{in} < A_{Fc} < I_{ci} $
S^1_{32} open	$A_{Fa} > I_{ai} $	$A_{Fb} > I_{bi} $	$A_{Fc} < I_{ci} _{ex}$
S^1_{33} open	$A_{Fa} > I_{ai} $	$A_{Fb} > I_{bi} $	$ I_{ci} _{in} < A_{Fc} < I_{ci} $
S^1_{34} open	$A_{Fa} > I_{ai} $	$A_{Fb} > I_{bi} $	$A_{Fc} < I_{ci} _{ex}$
Inductive Operation			
No fault	$A_{Fa} = I_{ar} $	$A_{Fb} = I_{br} $	$A_{Fc} = I_{cr} $
S^1_{11} open	$ I_{ar} _{in} < A_{Fa} < I_{ar} $	$A_{Fb} > I_{br} $	$A_{Fc} > I_{cr} $
S^1_{12} open	$A_{Fa} < I_{ar} _{ex}$	$A_{Fb} > I_{br} $	$A_{Fc} > I_{cr} $
S^1_{13} open	$A_{Fa} < I_{ar} _{ex}$	$A_{Fb} > I_{br} $	$A_{Fc} > I_{cr} $
S^1_{14} open	$ I_{ar} _{in} < A_{Fa} < I_{ar} $	$A_{Fb} > I_{br} $	$A_{Fc} > I_{cr} $
S^1_{21} open	$A_{Fa} > I_{ar} $	$ I_{br} _{in} < A_{Fb} < I_{br} $	$A_{Fc} > I_{cr} $
S^1_{22} open	$A_{Fa} > I_{ar} $	$A_{Fb} < I_{br} _{ex}$	$A_{Fc} > I_{cr} $
S^1_{23} open	$A_{Fa} > I_{ar} $	$A_{Fb} < I_{br} _{ex}$	$A_{Fc} > I_{cr} $
S^1_{24} open	$A_{Fa} > I_{ar} $	$ I_{br} _{in} < A_{Fb} < I_{br} $	$A_{Fc} > I_{cr} $
S^1_{31} open	$A_{Fa} > I_{ar} $	$A_{Fb} > I_{br} $	$ I_{cr} _{in} < A_{Fc} < I_{cr} $
S^1_{32} open	$A_{Fa} > I_{ar} $	$A_{Fb} > I_{br} $	$A_{Fc} < I_{cr} _{ex}$
S^1_{33} open	$A_{Fa} > I_{ar} $	$A_{Fb} > I_{br} $	$A_{Fc} < I_{cr} _{ex}$
S^1_{34} open	$A_{Fa} > I_{ar} $	$A_{Fb} > I_{br} $	$ I_{cr} _{in} < A_{Fc} < I_{cr} $

The lower the value $|I_a S^1_{xy}(f)|$, the effect is increased when the faulty STATCOM is under the capacitive operation and is sensitive compared to the inductive operation.

The application of the single-sided fundamental amplitude spectrum method presents an advantage since it has the ability to detect and localize the faulty switch of each leg separately. For example, if each of the switches (S^1_{13} , S^1_{21} , S^1_{34}) are faulty, then three different amplitude spectra are shown where each phase has a certain value, but in the case of the Park vectors method, any faulty switch cannot be determined. There are six values for the SSAS in the case of the healthy state of conv1. Note that all the phases, in this case, have the same amplitude spectrum value $|I_{ai}| = |I_{br}| = |I_{ci}|$. By cons, in the case of an open-circuit fault for example, if the value of $|I_{ai}|$ is reduced, the values of $|I_{br}|$ and $|I_{ci}|$ in the remaining two phases are increased which means that the fault occurred in the first leg and therefore here the faulty leg is directly localized.

In the second, the SSAS value is to be exactly calculated because it has four values, two large and two small, where the large values are external.

The flowchart shows the different steps of the switches and the other two are the internal switches as they are defined as $|I_{ai}|_{ex}$ and $|I_{ai}|_{in}$, here the faulty

switch is localized. Fundamental amplitude spectrum current value by the SSAS method is shown in Fig. 9.

5. Faulty Converter Reconfiguration

5.1. Reconfigured Faulty Converter Topology

According to Fig. 10, the structure of a three-level converter is considered and is changed by adding active switches to the converter clamping diodes where it is considered as a new application for the STATCOM. The importance of this change is to allow the restoration of the level of voltage loss in the case of open-circuit faults in addition to the appearance of bidirectional current paths [28]. The integration of the two NC relay types: (S^0_{U1} , S^1_{U1}, \dots) in each leg is to isolate the open-circuit fault. The importance of the relay (S_{NP}) is to isolate the Neutral Point (NP) during a failure mode. In order to protect the freewheeling diode fault problem, the SNP relay is linked at the neutral point to control the connection depending on the type of fault. For example, if there is a fault in the switch S^1_{11} in the first leg of conv1, the SNP relay opens for

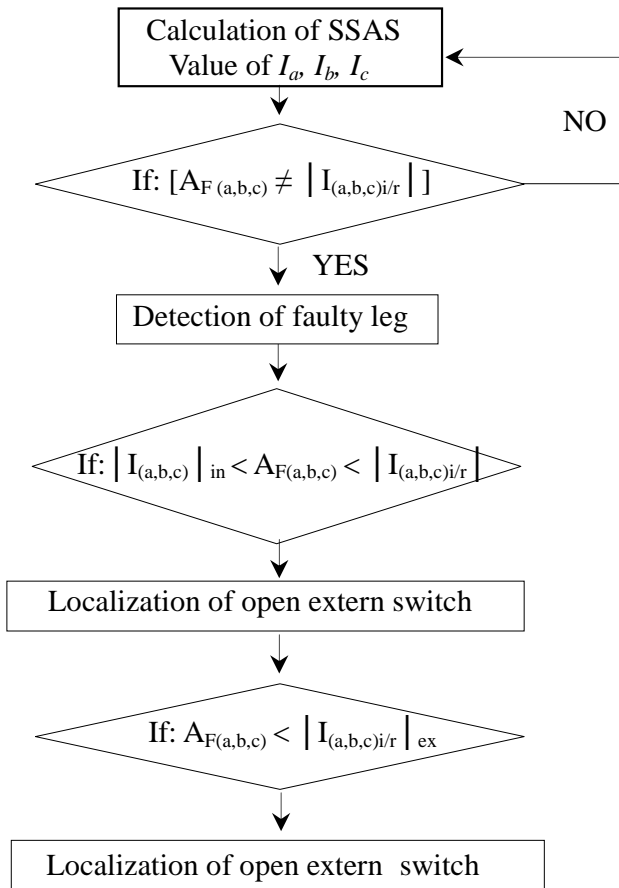


Fig. 9: Flowchart of the amplitude spectrum current value by SSAS method.

neutral point disconnection in order to allow the exploitation of alternative configurations. After completing the SNP opening, the converter will operate in an alternative mode to meet the required voltage in the faulty leg. Opening through SNP switching, the converter will operate in an alternative mode to meet the required voltage in the faulty leg.

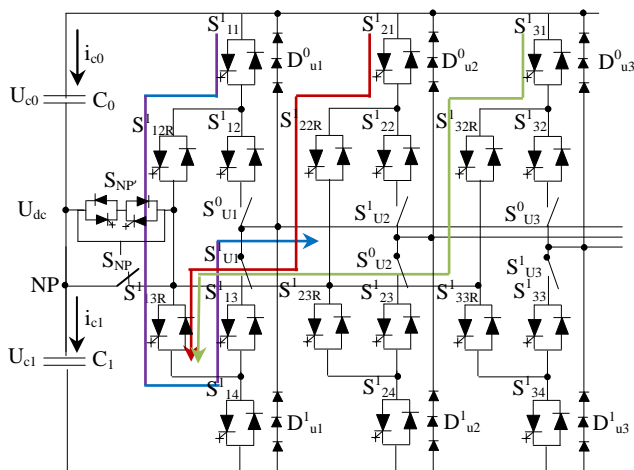


Fig. 10: Reconfiguration of three-level NPC converter.

6. STATCOM Control by Integrating Multi-Level Fault Tolerant Converters

This section tackles the STATCOM control through the application of multi-level fault tolerant converters. The reconfigurable fault tolerant is necessary to maintain and ensure service continuity of the STATCOM system. The general detailed structure of the reconfigurable multi-level fault tolerant converters with their diagnostic blocks is shown in Fig. 11. Each converter in the general structure is connected with three blocks;

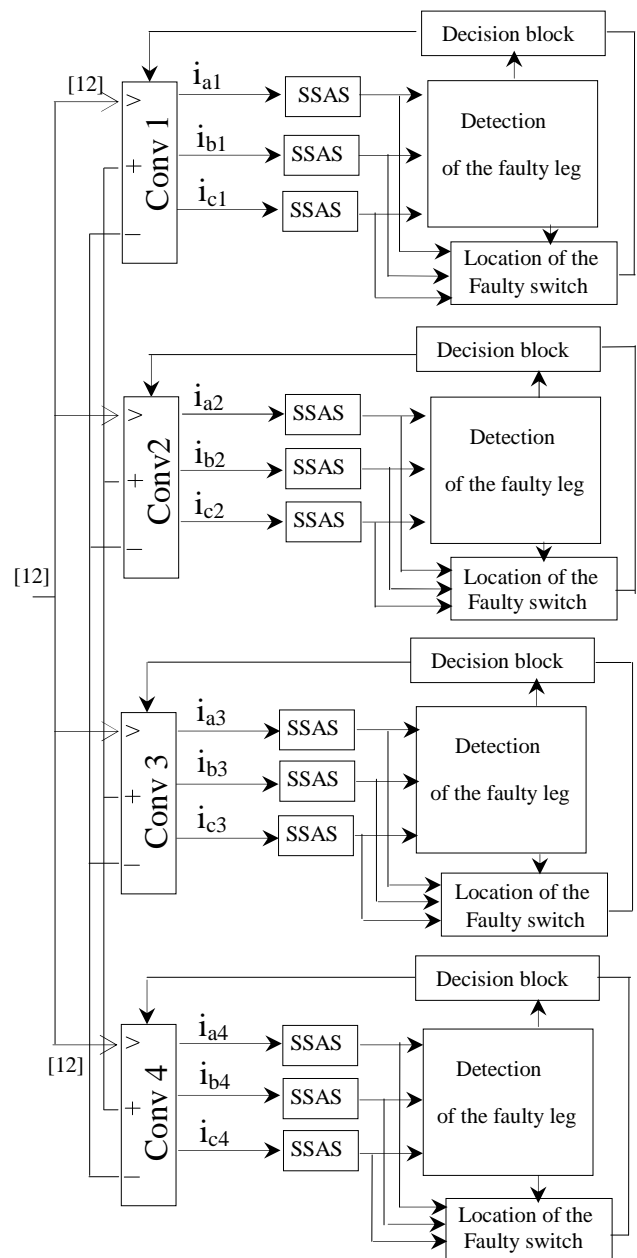


Fig. 11: General diagram of four fault-tolerant converters with their detection blocks and locations.

the first is to detect the faulty leg, the second is to localize the faulty switch, and the last block is for the re-configuration action which takes place once the fault is localized.

There are basically 12 currents which are all subject to spectral analysis simultaneously.

7. Simulation Results and Discussion

Figure 12 illustrates the fault tolerant converter performance in the STATCOM under the influence of the fault occurring in the two instants 0.5 s and 0.7 s and

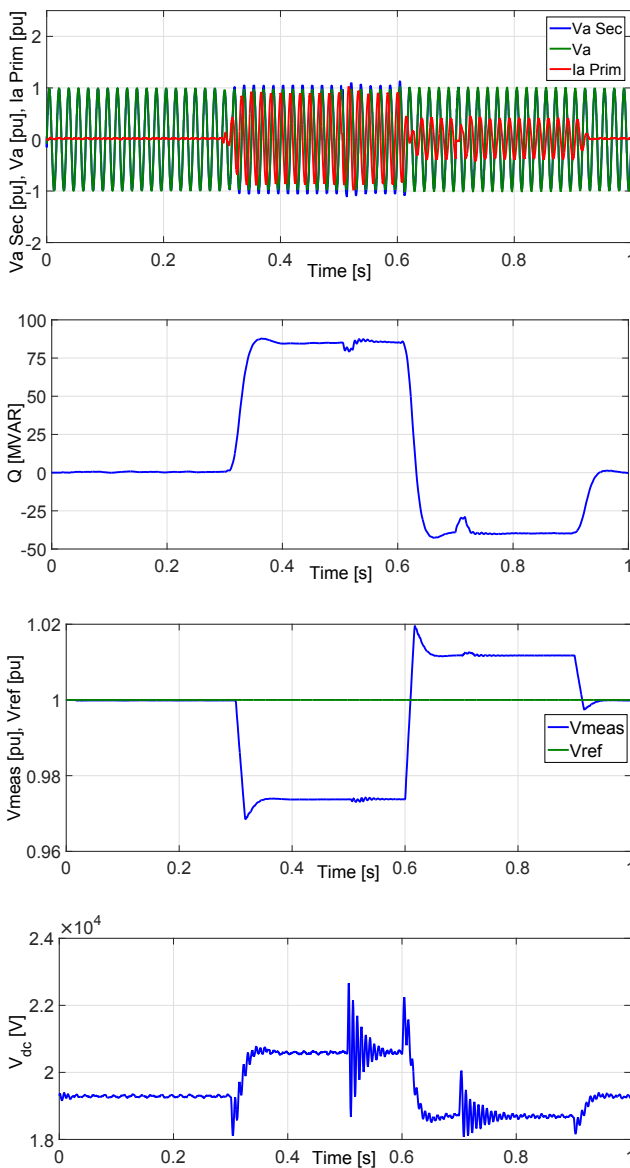


Fig. 12: Timeline of the healthy operation, the fault duration and the post-fault operation of an open-circuit fault introduced at GTO switch S112 of conv1.

its impact on the absorption or generation of the reactive power. The results obtained in Fig. 12, show that after the fault occurring at the instant 0.5 s, it results in a slight decrease in the reactive power Q followed by a slight increase at the instant 0.7 s.

After the re-configuration, the reactive power returned to its initial value. It should be noted that a slight distortion is visible at the level of the primary current I_a Prim at the instants 0.5 s and 0.7 s; then the current signal immediately returns to its initial sinusoidal form. Ripples also occurred in the DC voltage between 0.97 pu and 1.16 pu at 0.5 s and between 0.94 pu and 1.04 pu at 0.7 s; then immediately returns to its initial DC form. From all these presented results, it can be deduced that the integration of the three-level converter fault-tolerant has brought profitable solutions to the STATCOM system in terms of avoiding harmonics caused by current distortions as well as the amount of loss or excess of the reactive power.

In this last part of this section, as depicted by Fig. 13, two very important tasks are added to represent the isolation of the faulty switch and the re-configuration of the control strategy, which is to be added to the flowchart of Fig. 9, in order to ensure the process continuity of the entire STATCOM fault-tolerant system.

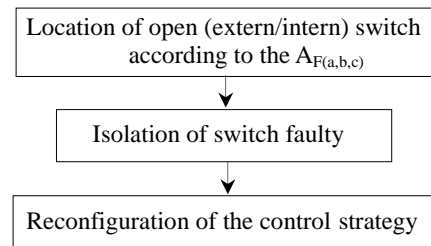


Fig. 13: Flowchart of the isolation and reconfiguration tasks for the faulty conv1.

Figure 14 shows the different instants before and after the fault occurrence. The time taken by the detection, localization and reconfiguration operations is 0.005 s, which is very short and sufficient enough to ensure the continuity of service of the STATCOM system.

8. The Fault Effect of the First Leg Switches on the Value of SSAS

In this case, an open-circuit fault is introduced in the first leg switches each one separately, in order to understand the effect of the voltage source changes on the value of SSAS in the faulty state under capacitive and

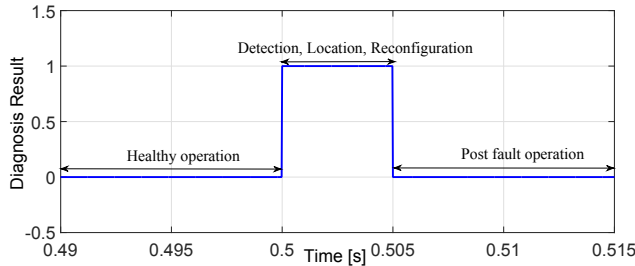


Fig. 14: Timeline of the healthy operation, the fault duration and the post-fault operation of an open-circuit fault introduced at GTO switch S^{1}_{12} of conv1.

inductive operation. In Fig. 13, under capacitive operation, it can be concluded that increasing the voltage source leads to reduction value of SSAS. With regard to the capacitive operation, the value of the SSAS increases in the interval [1.01–1.05] and stabilizes when the value exceeds 1.05 pu. From this finding, it can be deduced that the value of SSAS is affected by increasing the value of the voltage source under the capacitive operation mode more than that of the inductive operation mode.

According to Fig. 15, it should be noted that a difference in the values of THD between the internal switches (S^{1}_{12} , S^{1}_{13} , S^{1}_{22} , S^{1}_{23} , S^{1}_{32} and S^{1}_{33}) and external switches (S^{1}_{11} , S^{1}_{14} , S^{1}_{21} , S^{1}_{24} , S^{1}_{31} and S^{1}_{34}) is observed in the capacitive operating mode.

On the contrary, in the inductive operating mode, the values of THD are close.

It can be concluded from these results that the capacitive operating mode is more affected by the fault compared to that of the inductive operating mode. It

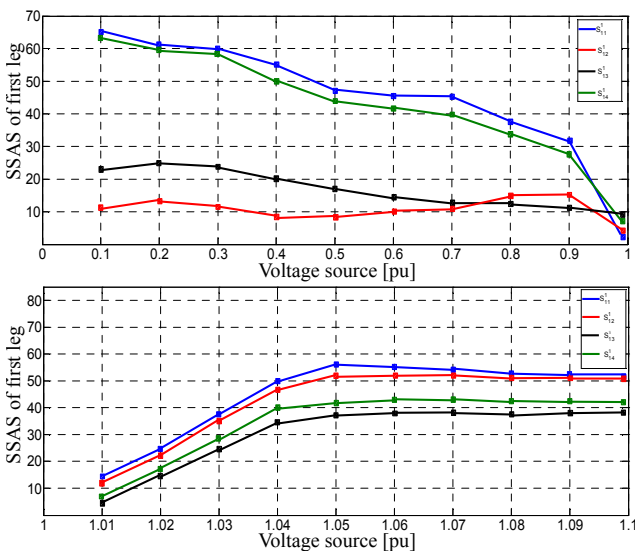


Fig. 15: Fundamental amplitude spectrum values behavior by changing the open-circuit fault of each first leg switch under capacitive and inductive operating modes.

also should be noted that the diagnosis becomes easier in the capacitive operating mode.

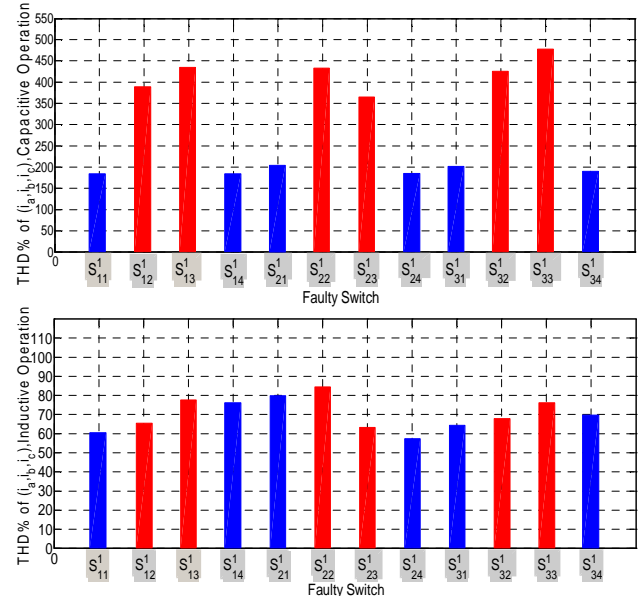


Fig. 16: THD values as percentage of 12 switches open-circuit faults for capacitive and inductive modes.

9. Conclusion

The paper addresses a very important issue related to the use of STATCOM in electrical networks and the required means to ensure continuity of service in case of converter switches open-circuit fault occurrence. The importance of this study is more justified by the fact that nowadays, the STATCOM system is very indispensable in electrical networks as it plays a key role in maintaining the network voltage based on the absorption or the generation of the reactive power.

First, the paperwork focuses on the STATCOM system in both the healthy and the faulty conditions by investigating the fault impact on network performance. In the healthy case, the STATCOM system is supporting and reinforcing the network. Whereas in the case of a converter fault, it becomes disabled and it influences negatively the network, making the value of the reactive power significantly reduced in the capacitive operating mode and increased in the inductive operating mode, in addition to the appearance of distorted currents.

The paperwork is then oriented towards the application of a diagnosis method to the STATCOM system based on the Single-Sided Amplitude Spectrum (SSAS). The important advantage of this method compared to Park vectors method, for example, is that it has the ability to diagnose each phase on its own hence facilitating the detection and localization process, espe-

cially in the case of faults in two operations (capacitive or inductive). From the findings of the SSAS diagnosis method, it is concluded that the faulty internal switches of the converter have more significant effects on the network system compared to the faulty external switches for the capacitive operating mode. By cons, for the inductive operating mode, the effect of all the faulty switches influences little the network system. It can be then deduced that the faulty converter in the capacitive operation is more sensitive compared to the inductive operation.

The last part of the paper is concerned with the integration of the three-level converter fault tolerance as a solution to ensure continuity of the STATCOM system. It is found that the very short time taken by the detection, localization, and reconfiguration operations is equal to 0.005 s, an acceptable value in comparison to other reported studies.

Acknowledgment

This work was supported by Research Center in Industrial Technologies CRTI, P.O.Box 64, Cheraga 16014, Algiers, Algeria crti.dz.

References

- [1] JOHNS, A. T., A. TER-GAZARIAN and D. F. WARNE. *Flexible ac transmission systems (FACTS)*. London: The Institute of Electrical Engineers, 1999. ISBN 0-85296-771-3.
- [2] HINGORANI, N. G. and L. GYUGYI. *Understanding FACTS: Concepts and Technology of Flexible AC Transmission Systems*. New York: Wiley-IEEE Press, 2000. ISBN 978-0470546802.
- [3] MATHUR, R. M. and R. K. VARMA. *Thyristor-Based FACTS Controllers for Electrical Transmission Systems*. New York: Wiley-IEEE Press, 2002. ISBN 0-471-20643-1.
- [4] PADIYAR, K. R. *FACTS Controllers in Power Transmission and Distribution*. New Delhi: New Age International Publishers, 2007. ISBN 978-81-224-2541-3.
- [5] HINGORANI, N. G. Power electronics in electric utilities: role of power electronics in future power systems. *Proceedings of the IEEE*. 1988, vol. 76, iss. 4, pp. 481–482. ISSN 0018-9219. DOI: 10.1109/5.4432.
- [6] GYUGYI, L., N. G. HINGORANI, P. R. NANNERY and N. TAI. Advanced Static Var Compensator Using Gate Turn-off Thyristors for Utility Applications. *CIGRE Paper no. 23-203*. 1990, pp. 1–8.
- [7] HINGORANI, N. G. and L. GYUGYI. *Understanding FACTS*. New York: IEEE Power Engineering Society and IEEE Press, 1999. ISBN 978-0780334557.
- [8] VORAPHONPIPUT, N., I. NGAMROO and S. CHATRATANA. Control System Design for a STATCOM using Complex Transfer Function. In: *6th International Conference on Instrumentation, Measurement, Circuits & Systems*. Hangzhou: WSEAS, 2007, pp. 186–192.
- [9] EL-MOURSI, M. S. and A. M. SHARAF. Novel controllers for the 48-pulse VSC STATCOM and SSSC for voltage regulation and reactive power compensation. *IEEE Transactions on Power Systems*. 2005, vol. 20, iss. 4, pp. 1985–1997. ISSN 0885-8950. DOI: 10.1109/TPWRS.2005.856996.
- [10] PADIYAR, K. R. and N. PRABHU. Design and performance evaluation of subsynchronous damping controller with STATCOM. *IEEE Transactions on Power Delivery*. 2006, vol. 21, iss. 3, pp. 1398–1405. ISSN 0885-8977. DOI: 10.1109/TPWRD.2005.861332.
- [11] BENAOUA, O. F., A. BENDIABDELLAH and B. D. E. CHERIF. Contribution to Reconfigured Multi-Level Inverter Fed Double Stator Induction Machine DTC-SVM Control. *International Review on Modelling and Simulations*. 2016, vol. 9, no. 5, pp. 1–13. ISSN 1974-9821. DOI: 10.15866/iremos.v9i5.10053.
- [12] ERTUGRUL, N., W. SOONG, G. DOSTAL and D. SAXON. Fault tolerant motor drive system with redundancy for critical applications. In: *33rd Annual IEEE Power Electronics Specialists Conference*. Cairns: IEEE, 2002. ISBN 0-7803-7262-X. DOI: 10.1109/PSEC.2002.1022381.
- [13] CIAPPA, M. Selected failure mechanisms of modern power modules. *Microelectronics Reliability*. 2002, vol. 42, iss. 4–5, pp. 653–667. ISSN 0026-2714. DOI: 10.1016/S0026-2714(02)00042-2.
- [14] HADIOUCHE, D., H. RAZIK and A. REZ-ZOUG. On the modeling and design of dual-stator windings to minimize circulating harmonic currents for VSI fed AC machines. *IEEE Transactions on Industry Applications*. 2004, vol. 40, iss. 2, pp. 506–515. ISSN 0093-9994. DOI: 10.1109/TIA.2004.824511.
- [15] ROTHENHAGEN, K. and F. W. FUCHS. Performance of diagnosis methods for IGBT open circuit

- faults in three phase voltage source inverters for AC variable speed drives. In: *European Conference on Power Electronics and Applications*. Dresden: IEEE, 2005, pp. 1–10. ISBN 90-75815-09-3. DOI: 10.1109/EPE.2005.219426.
- [16] FUCHS, F. W. Some diagnosis methods for voltage source inverters in variable speed drives with induction machines - a survey. In: *29th Annual Conference of the IEEE Industrial Electronics Society*. ROANOKE: IEEE, 2003, pp. 1378–1385. ISBN 0-7803-7906-3. DOI: 10.1109/IECON.2003.1280259.
- [17] CHERIF, B. D. E., A. BENDIABDELLAH and M. A. KHELIF. Detection of Open-Circuit Fault in a Three-Phase Voltage Inverter Fed Induction Motor. *International Review of Automatic Control*. 2016, vol. 9, no. 6, pp. 374–382. ISSN 1974-6059. DOI: 10.15866/ireaco.v9i6.10268.
- [18] MENDES, A. M. S. and A. J. M. CARDOSO. Fault Diagnosis in a Rectifier-Inverter System Used in Variable Speed AC Drives, by the Average Current Park's Vector Approach. In: *8th European Conference on Power Electronics and Applications*. Lausanne: EPE, 1999, pp. 1–9. ISBN 978-9075815047.
- [19] KIM, D.-E. and D.-C. LEE. Fault Diagnosis of Three-Phase PWM Inverters Using Wavelet and SVM. *Journal of power electronics*. 2009, vol. 9, iss. 3, pp. 377–385. ISSN 1598-2092.
- [20] LU, B. and S. K. SHARMA. A Literature Review of IGBT Fault Diagnostic and Protection Methods for Power Inverters. *IEEE Transactions on Industry Applications*. 2009, vol. 45, iss. 5, pp. 1770–1777. ISSN 0093-9994. DOI: 10.1109/TIA.2009.2027535.
- [21] LU, B. and S. K. SHARMA. A survey of IGBT fault diagnostic methods for three-phase power inverters. In: *International Conference on Condition Monitoring and Diagnosis*. Beijing: IEEE, 2008, pp. 1–8. ISBN 978-1-4244-1621-9. DOI: 10.1109/CMD.2008.4580396.
- [22] KHELIF, A. M., B. D. E. CHERIF and A. BENDIABDELLAH. Diagnosis of SVM Controlled Three-Phase Rectifier Using Mean Value of Park Currents Technique. *International Review on Modelling and Simulations*. 2018, vol. 11, iss. 2, pp. 93–101. ISSN 1974-9821. DOI: 10.15866/iremos.v11i2.13848.
- [23] MAVIER, R., F. RICHARDEAU and H. PIQUET. *Onduleur Reconfigurable, a Tolerance de Pannes, pour l'Alimentation d'un Moteur Triphase Synchrone a Aimants Permanents, et Ensemble Desdits Onduleur et Moteur*. Aux noms de Airbus France SAS, Centre National de Recherche Scientifique, Institut National Polytechnique de Toulouse, 2010. FR 2 892 243 B.
- [24] BOULON, L., D. HISSEL, A. BOUSCAYROL, O. PAPE and M.-C. PERA. Simulation Model of a Military HEV With a Highly Redundant Architecture. *IEEE Transactions on Vehicular Technology*. 2010, vol. 59, iss. 6, pp. 2654–2663. ISSN 0018-9545. DOI: 10.1109/TVT.2010.2045522.
- [25] BETTA, G., M. D'APUZZO, C. LIGUORI and A. PIETROSANTO. An intelligent FFT-analyzer. *IEEE Transactions on Instrumentation and Measurement*. 1998, vol. 47, iss. 5, pp. 1173–1179. ISSN 0018-9456. DOI: 10.1109/19.746578.
- [26] BETTA, G., C. LIGUORI and A. PIETROSANTO. A multi-application FFT analyzer based on a DSP architecture. *IEEE Transactions on Instrumentation and Measurement*. 2001, vol. 50, iss. 3, pp. 825–832. ISSN 0018-9456. DOI: 10.1109/19.930461.
- [27] IM, W.-S., J.-S. KIM, J.-M. KIM, D.-C. LEE and K.-B. LEE. Diagnosis methods for IGBT open switch fault applied to 3-phase AC/DC PWM converter. *Journal of power electronics*. 2012, vol. 12, iss. 1, pp. 120–127. ISSN 1598-2092. DOI: 10.6113/JPE.2012.12.1.120.
- [28] FERNANDO SILVA, J. and S. F. PINTO. *Control Methods for Switching Power Converters*. Chapter 34, pp. 935–998. San Diego: Academic Press, 2001. ISBN 0-12-581650-2.

About Authors

Omar Fethi BENAOUA was born on November 5th, 1984 in Tiaret, Algeria. He received the state engineer degree in electrical engineering from the University of Djelfa, Algeria in 2009, and his Magister degree from the University of Sciences and Technology of Oran, (USTO-MB) Algeria in 2013, and the Ph.D. degree in control of electrical drives and diagnostics in 2017. He is currently a lecturer of electrical engineering at the University of Djelfa. He is working with the Diagnostic Group, LDEE laboratory at University of Sciences and Technology of Oran since 2010. His research interests include electrical machines and drives control with application of artificial Intelligence: fuzzy logic and neuron network as well as multi-level inverters and fault tolerance.

Azzedine BENDIABDELLAH is IEEE Member from Algeria. He received his Bachelor Engineering degree with honours and his Ph.D. degree from the University of Sheffield, England, in 1980, and 1985 respectively. He is currently Professor Lecturer/Researcher and Director of the Laboratory of Development of Electrical Drives (LDEE) and Head of the Diagnostic Group in the Electrical Engineering Faculty at the University of Sciences and Technology of Oran Mohammed Boudiaf, (USTO-MB) Algeria. His research interests include electrical machines, Drives Modelling, and Analysis, Electrical machines, Drives Control and Converters as well as Electrical machines, Drives Faults Diagnosis, and Fault Tolerance.

Bilal Djamel Eddine CHERIF was born in Algeria in 1985. He received his Engineering degree from the University of M'sila, Algeria in 2010 and his Magister Degree in Electrical Engineering from the University of Sciences and Technology of Oran (USTO-MB), Algeria in 2015 respectively. He is currently working on his Ph.D. degree at USTO-MB, Algeria. His research interests include Power Conversion and Electric Machines and Drives and Fault Tolerance.

Appendix A Symbols:

a, b, c	Indexes corresponding to the three phases (a), (b), (c).
i, r	Indexes corresponding to the inverter and the rectifier.
A_F	Fundamental amplitude.
$ I_{ai} $	Fundamental amplitude of the first leg of the healthy inverter.
$ I_{ai} _{ex}$	Fundamental amplitude spectrum of the first leg of the faulty inverter (open-circuit of the external switch).
$ I_{br} _{in}$	Fundamental amplitude spectrum of the second leg of the faulty rectifier (open-circuit of the internal switch).
D_{ul}^0	Upper diodes of inverter first phase.
GTO	Gate Turn-Off thyristor.
NP	Neutral Point.
NPC	Neutral Point Clamped.
$SSAS$	Single-Sided Amplitude Spectrum.
S_{NP}	Relay to isolate neutral-point.
$S_{NP'}$	Bidirectional switch to connect/disconnect neutral-point.
S_{11R}^1	Series redundant device S_{11}^1 .
S_{ul}^0	Relay associated with the faulty first leg.
S_{12}^1	Internal switch of the first converter leg.
S_{31}^1	External switch of the third converter leg.